Title

TRIM11 is overexpressed in high-grade gliomas and promotes proliferation, invasion, migration and glial tumor growth

Journal

Oncogene, 32(42)

ISSN

0950-9232

Authors

Di, K

Linskey, ME

Bota, DA

Publication Date

2013-10-17

DOI

10.1038/onc.2012.531

Published in final edited form as:
Oncogene. 2013 October 17; 32(42): 5038–5047. doi:10.1038/onc.2012.531.

TRIM11 is over-expressed in high-grade gliomas and promotes proliferation, invasion, migration and glial tumor growth

Kaijun Di[1], **Mark E. Linskey**[1,3], and **Daniela A. Bota**[1,2,3,*]

Kaijun Di: kdi@uci.edu; Mark E. Linskey: mlinskey@uci.edu; Daniela A. Bota: dbota@uci.edu

[1]Department of Neurological Surgery, UC Irvine School of Medicine, Orange, CA, 92868, USA

[2]Department of Neurology, UC Irvine School of Medicine, Orange, CA, 92868, USA

[3]UC Irvine Chao Family Comprehensive Cancer Center, Orange, CA, 92868, USA

Abstract

TRIM11 (tripartite motif-containing protein 11), an E3 ubiquitin ligase, is known to be involved in the development of the central nervous system. However, very little is known regarding the role of TRIM11 in cancer biology. Here, we examined the expression profile of TRIM11, along with two stem cell markers CD133 and nestin, in multiple glioma patient specimens, glioma primary cultures derived from tumors taken at surgery, and normal neural stem/progenitor cells (NSCs). The oncogenic function of TRIM11 in glioma biology was investigated by knockdown and/or over-expression *in vitro* and *in vivo* experiments. Our results showed that TRIM11 expression levels were up-regulated in malignant glioma specimens and in high-grade glioma-derived primary cultures, while remaining low in glioblastoma multiforme (GBM) stable cell lines, low-grade glioma-derived primary cultures, and NSCs. The expression pattern of *TRIM11* strongly correlated with that of *CD133* and *nestin*, and differentiation status of malignant glioma cells. Knockdown of TRIM11 inhibited proliferation, migration and invasion of GBM cells, significantly decreased EGFR levels and MAPK activity, and down-regulated *HB-EGF* mRNA levels. Meanwhile, TRIM11 over-expression promoted a stem-like phenotype *in vitro* (tumorsphere formation) and enhanced glial tumor growth in immunocompromised mice. These findings suggest that TRIM11 might be an indicator of glioma malignancy, and has an oncogenic function mediated through the EGFR signaling pathway. TRIM11 over-expression potentially leads to a more aggressive glioma phenotype, along with increased malignant tumor growth and poor survival. Taken together, clarification of the biological function of TRIM11 and pathways it affects may provide novel therapeutic strategies for treating malignant glioma patients.

Keywords

TRIM11; oncogene; EGFR; malignant glioma; tumor formation

Introduction

Malignant gliomas are the most common primary tumors in the central nervous system, and are characterized by rapid cell proliferation, high invasiveness, genetic alteration, and increased angiogenesis (1). Despite continued advances in surgical and medical therapeutics,

*Corresponding Author: Dr. Daniela A. Bota, UC Irvine Medical Center, 101 The City Drive South, Shanbrom Hall, Suite 121, Orange, CA, 92868, Phone: 714-456-7032, Fax: 714-456-6894.

Conflict of interest

The authors declare no conflict of interest.

the prognosis for patients diagnosed with the most common and aggressive malignant glioma --glioblastoma multiforme (GBM)--remains poor, with a median survival of only 12–15 months (2).

In recent years, glioma molecular markers such as *MGMT* (O^6-methylguanine-DNA methyltransferase), *EGFR* and *IDH1* (isocitrate dehydrogenase-1) have played important roles in profiling the diagnosis, prognosis, and disease management in subtypes of glioma patients (2, 3). More recently, CD133 (prominin-1) and nestin have been considered as prognosis markers for glioma patients since their expression is associated with poor prognosis and correlates better with clinical course than the histological grading (4, 5). They are also used as markers for glioma stem-like cells (GSCs), a small subset of tumor cells situated at the apex of the cellular differentiation hierarchy, and responsible for sustaining long-term tumor growth through self-renewal and the production of more differentiated daughter cells (6–8). GSCs are known to contribute to tumorigenesis and radiation resistance in malignant glioma (9), and are regulated via many signaling pathways including Notch, Hedgehog, and MAPK cascades, *etc* (10). Due to the malignancy-driving roles of GSCs, drugs that specifically targeting the GSCs have a very important potential role in glioma therapy (11). However, both CD133 and nestin are also present on non-malignant neural stem/progenitor cells (NSCs) (12, 13), and targeting GSCs through these markers will likely damage NSCs. This is particularly problematic in the brain, since damage to NSCs resulting from glioma therapies (14) can produce profound cognitive side effects that impair patient functional independence and quality of life (15, 16).

The tripartite motif-containing (TRIM) family is characterized by unique structural motifs: a RING finger domain, a B-box domain and a coiled-coil domain, making them members of the RING B-box coiled-coil (RBCC) protein family (17–19). Members of this family have been implicated in various cellular processes, including development, neurodegenerative diseases, cellular response to viral infection and cancer (20). As a 3 typical RBCC protein, TRIM11 functions as an E3 ubiquitin ligase, and binds to and destabilizes Humanin (HA), a neuroprotective peptide against Alzheimer's disease-relevant insults (21). In addition, TRIM11 interacts with and destabilizes the activator-mediated cofactor complex (ARC105), which in turn suppresses ARC105-mediated transcriptional activation induced by transforming growth factor β (TGF-β) signaling (22). TRIM11 also binds to and mediates the ubiquitination of PAX6 (paired box 6), a member of the PAX family of transcription factors and plays a key role in organogenesis of the eye, pancreas, and brain (23). Finally, TRIM11 is involved in the specification of noradrenergic (NA) phenotype by interacting with Phox2b, a homeodomain transcription factor that could modulate development of NA neurons (24). These findings implicate an important, albeit still incompletely defined, role of TRIM11 in nervous system function and development. Nonetheless, an oncogenic function of TRIM11 has yet to be identified in cancer cells of glial origin which shares a lot of common characteristics with the normal glial cells of the brain (25). In this study, we not only provide evidence that TRIM11 expression levels correlate with the malignancy of glioma, but also investigate the oncogenic function of TRIM11 *in vitro* and *in vivo*.

Results

TRIM11 is over-expressed in human high-grade glioma tumors and glioma-derived GSCs but not in NSCs, low-grade glioma-derived GSCs or stable malignant glioma cell lines

To investigate the correlation between TRIM11 and malignancy of glioma, immunohistochemical analysis of TRIM11 was performed using patient-derived glioma samples (Figure 1a). Strong TRIM11 staining was detected in GBM tissues, but much less in Grade II tissues and normal brain (representative results shown). Next, we profiled *TRIM11* mRNA levels using nineteen diverse histological primary GSCs derived from glioma

patients (Table 1), four stable GBM cell lines (U-251, D-54, LN-229 and U-87), and three NSCs (SC23, SC27 and SC30). Overall, *TRIM11* was low in all GBM cell lines, 6 of 7 (85.7%) low grade-GSCs, and all NSCs (normalized fold expression <2.5). By comparison, 1 of 3 (33.3%) Grade III-GSC and 7 of 9 (78%) GBM-GSCs had higher levels of *TRIM11* (normalized fold expression >2.5, Table 1 and Supplementary Figure 1a). The expression pattern of TRIM11 in cells was further confirmed at the protein levels. Western blotting data showed that TRIM11 expressed higher in GBM-GSCs (Supplementary Fig 1b), consistent with its mRNA levels. To evaluate the role of TRIM11 on clinical prognosis, we compared the outcome of patients with different expression levels of *TRIM11.* As shown in Table 1 (survival data), the high-grade glioma patients with lower *TRIM11* had a better prognosis (average 13.5 month survival for GBM patients) compared to patients with higher *TRIM11* (average 7.3 month survival for GBM patients).

Next, we compared *TRIM11* mRNA levels to those of *CD133.* Consistent with a previous report (26), the three NSC cultures displayed excessively high *CD133* (up to 3000-fold normalized expression). While all stable GBM cell lines and low-grade glioma-derived GSCs (except DB51) showed very low *CD133*, *CD133* was strongly expressed in all GBM-GSCs, and in one Grade III-GSC (Table 1 and Supplementary Figure 1a). Our results were consistent with previous reports (4, 5) that high *CD133* mRNA levels correlate with glioma malignancy. More importantly, GSCs having elevated *TRIM11* expressed concurrently higher *CD133* (shading in Table 1). For example, the two GBM-GSCs (DB32 and HuTuP01) that showed the highest levels of *TRIM11* (29.25-fold and 13.78-fold, respectively) also displayed the highest levels of *CD133* (66.07-fold and 27.34-fold, respectively), indicating a positive correlation between *TRIM11* and *CD133* in gliomas. Next, we performed immunofluorescent double staining to further compare the expression parallel between CD133 and TRIM11 using corresponding tissue sections. As shown in Figure 1b, both DB44 (Grade II) and DB32 (GBM) revealed co-expression of TRIM11 and CD133, but the strong immunopositivity was detected only in DB32. HuTuP01-GSC was used to confirm these data. As shown in Figure 1c, TRIM11 was localized diffusely mainly in the cytoplasm but also in the nucleoplasm (top), which was consistent with previous reports (17, 22), and strongly expressed on tumorsphere (bottom). Meanwhile, the cells positive for TRIM11 staining also displayed strong CD133 immunopositivity in both tumorsphere and monolayer cells.

For *nestin* expression study, U-251 was used as a positive control as previous described (27). Our results showed that *nestin* expressed at elevated levels in almost all glioma-drived GSCs tested and more robustly in all GBM-GSCs and NSCs (Table 1 and Supplementary Figure 1a).

Taken together, our results suggest that the levels of TRIM11 correlate with the malignancy of glioma and potentially with glioma patient prognosis. Compared to CD133 and *nestin*, TRIM11 might be a more specific indicator for GSCs since it is up-regulated only in malignant glioma-derived GSCs, but not in NSCs or low-grade glioma-derived GSCs.

TRIM11 mRNA levels correlate with differentiation status and *CD133* mRNA levels in gliomas

When cultured in serum-free medium, which allows for the maintenance of an undifferentiated stem cell state, glioma cells form tumorspheres, along with an increased expression of CD133 (28, 29). To further investigate the correlation between *TRIM11,* differentiation status and *CD133* expression levels in gliomas, we used serum-free stem cell medium (SCM) to culture the stable glioma cell line D-54, and measured the changes in *TRIM11* and *CD133* mRNA levels by qRT-PCR. When cultured in 10% FBS-containing medium (differentiation medium), D-54 grew as a monolayer and attached to the culture

flask (Supplementary Figure 2a, left photo). After re-seeding in SCM, they grew as typical tumorspheres varied in size and floating in the medium (Supplementary Figure 2a, right photo). In addition, both *TRIM11* and *CD133* were increased when cells were cultured in SCM (Figure 2a), suggesting that D-54 cells cultured in stem cell conditions can achieve the properties classically ascribed to GSCs, and confirming again a positive correlation between *TRIM11* and *CD133*. Next, using two GBM-GSCs which expressed highest *TRIM11* and *CD133* (DB32-GSC and HuTuP01-GSC), we switched culture media from SCM to differentiation medium to induce GSC differentiation. Accompanying with morphology changes (Supplementary Figure 2b and c), *TRIM11* and *CD133* significantly decreased when GSCs underwent differentiation [Figure 2b and c (left panel)]. Furthermore, when HuTuP01-GSC was switched back to SCM (leading to a less differentiated state), both *TRIM11* and *CD133* increased again (Figure 2c, right panel), and the morphology of the cells changed back to that of the cells cultured directly in SCM (Supplementary Figure 2c). By comparing with early and late passages of DB32-GSC and HuTuP01-GSC, we found both *TRIM11* and *CD133* decreased after continuous expansion (Figure 2d), further confirming that *TRIM11* levels are correlated with differentiation status and *CD133* levels of GSCs. The stem cell character of HuTuP01-GSC was further identified by differentiation assay (Supplementary Figure 2d), confirming their multipotential nature.

Down-regulation of TRIM11 suppresses proliferation, migration and invasion of glioma cells, and inhibits EGFR expression, MAPK signaling pathway, and transcription of *HB-EGF* and *CCND1*

To investigate the potential oncogenic function of TRIM11 in glioma, we knocked down TRIM11 in glioma cells through RNA interference. Both protein and mRNA levels of TRIM11 were decreased in *si*TRIM11 transfectants (Supplementary Figure 3a and b). We next investigated the effect of TRIM11 on cell proliferation using D-54. MTT assay (Figure 3a, upper panel) and BrdU cell proliferation analysis (Figure 3a, lower panel) indicated that loss of TRIM11 was able to significantly inhibit cell proliferation. Cell cycle analysis further showed that down-regulation of TRIM11 led to increased G1 phase cells and decreased S phase cells (Supplementary Figure 3c).

The invasive behavior of malignant gliomas limits the effectiveness of local therapies and contributes to their poor prognosis (30). Therefore, wound closure assay (Figure 3b) was performed to compare the migration capability between controls and TRIM11 knockdown U-251 cells. TRIM11 down-regulating cells displayed a slower migration capability than control: while control cells were able to migrate in and fill up the gap in 30 hours, the gap was only partially filled in *si*TRIM11 transfectants at the same time. Similar results were found in LN229 cells (Supplementary Figure 4a). The role of TRIM11 on cell invasion was next measured using the Matrigel invasion chamber assay (Figure 3c). In both D-54 and U-251 cells, suppression of TRIM11 inhibited cell invasion and the difference was statistically significant ($P<0.05$).

In GBMs, amplification and/or mutation of the gene encoding EGFR occurs in up to 60% of tumors and the constitutive activation of EGFR can promote glioma cell proliferation and invasion (31). As one of the main intracellular protein cascades of EGFR, deregulated MAPK pathway due to activation of EGFR will influence a diverse array of vital cellular functions such as proliferation, survival and differentiation (32, 33). We next evaluated the expression levels of EGFR and phosphorylation status of MAPK in glioma cells having different TRIM11 levels. As shown in Figure 3d and Supplementary Figure 4b, down-regulation of TRIM11 led to decreased expression of EGFR, p-c-Raf, p-MEK1/2, and p-44/42MAPK, suggesting that TRIM11 might regulate the EGFR/MAPK pathway. Meanwhile, PI3K-AKT signaling, another downstream of EGFR, was not affected by TRIM11 (Supplementary Figure 4c).

Next, we used the human EGF/PDGF signaling PCR array to study whether TRIM11 differentially regulate the transcription of any genes in the EGF/PDGF signaling pathway. Table 2 showed the profile of various differentially expressed genes with fold changes of 2 or higher. There were 6 up-regulated and 5 down-regulated genes in D-54 *si*TRIM11 (*si*-4) transfections, and 1 up-regulated and 4 down-regulated genes in U-251 *si*TRIM11 (*si*-4) transfections. Among all the genes changed, down-regulation of two genes, *HB-EGF* (Heparin-binding EGF-like growth factor) and *CCND1* (Cyclin D1), was found in both cell lines. Meanwhile, the expression of *EGFR* was not significantly changed. To confirm these results, we measured again mRNA levels of *EGFR*, *HB-EGF* and *CCND1* using different primers (Figure 3e). Our results showed that both *HB-EGF* and *CCND1* were dramatically decreased, while there was no statistically difference on *EGFR* in *si*TRIM11 transfectants. Similar results were found in LN229 cells transfected with three different *si*TRIM11s (Supplementary Figure 4d).

To compare with knockdown experiments, gain of function studies were further performed. Following transfection of a Flag-Trim11 construct (Supplementary Figure 5a), both the levels of EGFR and the activity of MAPK pathway were increased (Supplementary Figure 5b), further confirming an oncogenic function of TRIM11 through promoting the accumulation of EGFR and activity of MAPK cascade.

Over-expression of TRIM11 promotes tumorsphere formation and proliferation *in vitro* and tumor growth in vivo

To further test the oncogenic function of TRIM11 both *in vitro* and *in vivo*, transient and stable TRIM11 over-expressing transfectants (pDsRed2-Trim11) were generated using mouse GL261 glioma cells. Expression of *TRIM11* mRNA was analyzed in Figure 4a (stable transfection) and Supplementary Figure 5c (transient transfection). Consistent with our TRIM11 knockdown results, increased *HB-EGF* mRNA revealed in both transient (Supplementary Figure 5c) and stable (Supplementary Figure 5d) TRIM11 over-expressing cells. Interestingly, large tumorspheres were detected in stable pDsRed2-Trim11 cells, but not control cells (Figure 4a, right). This morphological change supports our hypothesis that TRIM11 plays an important role in achieving/maintaining the stem cell state and led us to test the sphere formation capability induced by up-regulation of TRIM11. As shown in Figure 4b, over-expression of TRIM11 significantly promoted tumorsphere formation (upper panel), and the size of spheres driven from pDsRed2-Trim11 cells was significantly larger than that of control cells (right). Meanwhile, cell proliferation rate was dramatically increased in pDsRed2-Trim11 cells when cells grew on Matrigel-coated surface (Figure 4b, lower panel).

Based on our *in vitro* data (which suggest that TRIM11 significantly increases glioma cell proliferation and invasion), we then tested whether TRIM11 over-expression can promote glioma growth *in vivo*. Stable pDsRed2-Trim11-GL261 cells and control cells were injected s.c. into BALB/C nu/nu mice. The tumors generated by the pDsRed2-Trim11-GL261 cells were more than three times larger (both tumor volume and weight) than the tumors generated by the control cells (Figure 4c and d). Furthermore, macroscopic examination of these tumors showed increased vascularization and extensive areas of necrosis-characteristics well described to predict an aggressive phenotype in glial tumors. These findings further support that TRIM11 over-expression enhances glioma cell ability to form aggressive tumors, and correlate with our findings in human specimens, where high TRIM11 levels correlated with poor prognosis.

Discussion

Significant progress has been made on investigating the cellular, molecular, and genetic changes involved in malignant gliomas aggressive biological behavior, treatment resistance and poor survival. Recently, identifying and targeting the GSCs has been considered as a powerful tool for developing therapeutic strategies, since GSCs are chemo- and radiotherapy resistant and possess self-renewal, differentiation, and multi-potentiality, leading to therapy failure and recurrence (8, 9, 34). However, this is a difficult task as majority of the GSC markers described to date, such as CD133 and nestin, are also present at similar or higher levels in the adult neural stem cells. Thus a cancer therapy targeted using these ubiquitous and non-specific markers would risk eradicating reserves of normal self-renewing neural stem cells. Furthermore, animals with decreased neurogenesis have impaired performance on hippocampus-dependent learning tasks (35), suggesting that ablation of NSCs in the course of glioma therapy might lead to undesirable cognitive side-effects.

Here, we provided evidences that TRIM11 may act as a novel marker for malignant gliomas. *TRIM11* expression levels correlated with the glioma malignancy, similar to those of *CD133* and *nestin*--- whose expression levels are indicators for grade levels of gliomas, and are well-published as prognostic markers (4, 5). More importantly, high TRIM11 were detected only in malignant glioma-derived GSCs and tissue sections (Table 1, Fig 1a and Supplementary Figure 1), suggesting that TRIM11 has the potential to become a specific GSC marker. In addition, *TRIM11* levels, concurrent with *CD133*, were associated with differentiation status of cells (Figure 2). Concurrence between TRIM11 and CD133 not only occurred at mRNA levels, but also at patterns of protein expression in cells. Co-expression of these two proteins was detected in both tissue sections (Figure 1b) and GSCs (Figure 1c). Interestingly, even though CD133 is a cell surface marker, immunofluorescence staining of CD133 generally shows a diffused cytoplasmic staining in our study and others (36, 37), possibly due to permeabilization of the cell membranes by fixative that inadvertently damage surface marker antigens (38).

We not only demonstrated for the first time that TRIM11 acts as a malignant glioma marker, but provided evidences that TRIM11 may exert its oncogenic function through promoting cell proliferation (Figs. 3a, 4b and Supplementary Figure 3c), migration (Figure 3b and Supplementary Figure 4a) and invasion (Figure 3c). Most importantly, our results indicated that TRIM11 exerts its effect through EGFR oncogenic pathway. A decreased expression of EGFR and weakened activity of Raf/MEK/ERK1/2 MAPK pathway were found in TRIM11 knocked down GBM cells (Figure 3d and Supplementary Figure 4b), which harbor the wild-type *EGFR* gene (39). In contrast, over-expressing TRIM11 increased the expression of EGFR and enhanced the activity of MAPK pathway (Supplementary Figure 5b).

HB-EGF is a heparin-binding member of the EGF family (40), and is up-regulated in response to oncogenesis (41, 42). Co-expression of HB-EGF with the amplified EGFR has been found in malignant gliomas, resulting in the formation of an autocrine loop (43). By binding and activating EGFR, HB-EGF in turn triggers EGFR downstream signaling pathways including MAPKs, which then induce a rapid and sustained induction of *HB-EGF* mRNA expression and secretion of HB-EGF (44). Besides being a ligand for EGFR, HB-EGF also induces the expression of matrix metalloproteinases MMP-9 and MMP-3, and elevates activation of cyclin D1 promoter (45), suggesting a role of HB-EGF as a potent inducer of tumor growth and angiogenesis. In our study, while the mRNA levels of *EGFR* were not affected by TRIM11 down-regulation, a significant decrease on *HB-EGF* and *CCND1* mRNA levels was detected in TRIM11 knock-down cells (Table 2 and Figure 3e). By comparison, over-expression of TRIM11 increased the *HB-EGF* mRNA levels (Supplementary Figure 5c and d). Further studies will be needed to identify: (1) whether

TRIM11 directly regulates the transcription of *HB-EGF* and/or *CCND1,* or alternatively, down-regulation of *HB-EGF* is a consequence of reduced EGFR levels and weakened MAPK pathway; or (2) whether TRIM11 may modulate the process of EGFR ubiquitination and degradation.

Finally, we provided evidence for the first time that over-expression of TRIM11 promotes tumorsphere formation *in vitro* and tumor growth *in vivo* (Figure 4). These *in vivo* results further support the hypothesis that TRIM11 over-expression predicts the development of large, vascular and necrotic tumors associated with poor prognosis.

In summary, our study profiles the gene expression pattern of *TRIM11* in various grade glioma specimens, as well as multiple GSCs, stable serum-grown glioma cell lines and NSCs, and finds a strong positive correlation among *TRIM11, CD133*, and *nestin* in high-grade GSCs. In addition, we investigated the oncogenic function of TRIM11 on proliferation, migration and invasion, demonstrating that TRIM11 may modulate EGFR expression and MAPK pathway, and bring the first evidence that TRIM11 over-expression promotes glial tumor growth *in vivo*. This finding expands our knowledge of the TRIM11 biology from its known roles in normal brain development and Alzheimer's neurotoxicity into cancer biology, while opening the door for a novel new area of glioma biology study with the potential to identify new translational targets and/or strategies.

Materials and Methods

Glioma tissues, cells and media

Institutional Review Board approval was obtained at University of California Irvine Medical Center and Children's Hospital of Orange County. Surgical specimens of brain tumors (Table 1) were obtained from patients who had undergone tumor resection with the neuropathological review completed by a specialty neuropathologist. NSCs (SC23, SC27, SC30) were derived from brains of premature neonates by Dr. Philip Schwartz (26). HuTuP01 GBM-GSCs were a gift from Dr. David Panchision (Children's National Medical Center) (46). As previously described (14), both NSCs and GSCs were cultured in undifferentiated conditions on Matrigel-coated dishes in 1:1 DMEM:F12 medium (Irvine Scientific), containing 10% BIT9500 (Stem Cell Technologies), 292 μg/mL glutamine (Irvine Scientific), 40 ng/mL FGF, 20 ng/mL EGF, and 20 ng/mL PDGF. For expansion, one-half of this medium was replaced every other day, and the cultures were passaged every seven days or when confluent using Non-enzymatic Cell Dissociation Solution (Sigma). All our GSCs are able to form spheres when grown on non-adherent surfaces. The GSCs express GFAP when they are grown under conditions favoring glial differentiation, and βIII-tubulin when they are grown under conditions favoring neural differentiation, confirming their multipotential nature (Supplementary Figure 2d).

The stable human glioma cell lines D-54 MG and U-251 MG were gifts from Dr. Darrell Bigner (Duke University, Durham, NC), LN229 was obtained from Dr. Martin Jadus (VA Long Beach Hospital), and U-87 MG as well as mouse cell line GL261 were gifts from Dr. Florence Hofman (University of Southern California). All the differentiated malignant glioma cell lines were cultured in a high glucose 1:1 DMEM/F12 medium (Irvine Scientific) containing 2 mM L-glutamine (Gibco/Invitrogen), 10% FBS (Omega Scientific, Inc.) and 1% penicillin/streotomycin (Gibco/Invitrogen). All cells were cultured at 37°C in a humidified incubator with 5% CO_2.

Quantitative RT-PCR (qRT-PCR) analysis

Total RNA was extracted using RNeasy Mini Kit (Qiagen), and cDNA was generated using the iScript™ cDNA Synthesis Kit (Bio-rad). Quantitative PCR reactions (iQ™ SYBR Green

Supermix, Bio-rad) were conducted using a Bio-Rad CFX96 Real-time System, and the gene expression levels were normalized to those of *ACTB*. The primers were described in Supplementary Methods.

Immunohistochemical and immunofluorescent staining

VECTASTAIN ABC kit (Vector Laboratories., Inc.) was used for immunohistochemical staining. Formalin-fixed, paraffin-embedded tissue sections (5μm) were deparaffinized and rehydrated. After antigen retrieval, the endogenous peroxidase activity was blocked with 1% H_2O_2 in PBS for 20 min. The sections were incubated with 5% normal goat serum and then exposed to rabbit anti-TRIM11 antibody (1:40, ProteinTech Group, Inc.) at 4 °C overnight, followed by incubation with biotinylated anti-rabbit IgG for 1 hour at room temperature, and counterstained by hematoxylin and eosin. Slides were then mounted with Permount (Fisher Scientific). For immunofluorescent double staining, the cells or tissue sections were first incubated with rabbit anti-TRIM11 and FITC-conjugated anti-rabbit secondary antibody (Millipore), and then CD133/1 (AC133)-PE antibody (Miltenyi Biotec Inc.), Nuclei were counterstained with DAPI (4′-6-diamidino-2-phenylindole) and slides were mounted with IMMU-MOUNT (Thermo Scientific).

*si*TRIM11 transfection

Four human FlexiTube *si*RNAs targeting *TRIM11* (SI00153230, SI00153237, SI00153244 and SI00153251) and negative control *si*RNA (1022076) were purchased from Qiagen, and were transfected into cells using HiPerFect transfection reagent (Qiagen). One *si*TRIM11 (*si*-4) was found to knockdown *TRIM11* expression most efficiently and was used in most of experiments.

Plasmid construction and transient and/or stable transfection assay

pcDNA3.1/Zeo Flag-Trim11 and pDsRed2-Trim11 were gifts from Dr. Seok Jong Hong (Northwestern University). Briefly, mouse brain mRNA was used to amplify full length *TRIM11* by RT-PCR followed by cloning into pcDNA3.1/Zeo vector and pDsRed2-C1 vector (24). Transfection was performed using FuGene 6 (Roche). For transient transfection, the cells were analyzed 72 hours after transfection. For generation of stable transfectants, the cells were selected by 0.4mg/ml of G418 (InvivoGen) for two weeks.

Western blotting

Antibodies with detailed descriptions were provided in Supplementary Methods. The images were exposed by KODAK M35A X-OMAT Processor.

BrdU cell proliferation analysis

Cell proliferation rates were determined by BrdU incorporation according to the manufacture's recommendation (Calbiochem). Briefly, the cells were incubated with BrdU Label for 24 hours, and then fixed. Monoclonal anti-BrdU antibody was added, followed by peroxidase-conjugated secondary antibody. The BrdU incorporation was measured at dual wavelengths of 450 and 570 nm, using a Model 680 Microplate Reader (Bio-Rad).

3-[4,5-Dimethylthiazol-2-yl]-2,5-diphenyltetrazolium bromide (MTT) assay

Cells (6×10^3/well) were seeded into 96-well plates. Before testing, MTT solution (5 mg/ml; 20 μl/well) was added and cells were incubated at 37 °C for 5 hours. The culture medium was then aspirated and DMSO (200 μl/well, Fisher Scientific) was added to dissolve the dark blue crystals. The absorbance was measured at a wavelength of 570 nm.

Wound closure assay

Cells were plated in 6-well plates and grew to full confluency. Similar sized wounds were then induced to monolayer cells by scraping a gap using a micropipette tip. After removing cell debris by rinsing with PBS, fresh medium was added and cells started migrating from the edge of the wound and repopulated the gap area. The time required for 'wound closure' was monitored and photographed immediately after wound incision and at indicated time points.

Invasion assay

Invasion assay was performed using BD BioCoat™ Matrigel™ Invasion Chamber with 8 μm PET membrane (BD Biosciences). Cells were seeded in medium without serum, and medium containing 1.5% FBS was used as chemoattractant. After an incubation of 24 hours at 37°C, non-invasive cells were removed and invading cells were fixed with 100% methanol. Cells were then stained in Hematoxylin.

Human EGF/PDGF signaling PCR array

Human EGF/PDGF signaling PCR array of 84 genes (SABiosciences, Qiagen) was performed according to the manufacturer's instructions. One μg of total RNA was used to synthesize cDNA. The manufacturer's web-based software package was utilized to calculate fold changes. Genes with greater than 2 fold differences were considered as significant.

Tumorsphere formation assay

Cells were plated at low density (500/well) in 6-well ultra-low attachment plates (Corning). After two weeks of culture, the number of floating tumorspheres in each well (diameter >50 μm) was counted.

Tumorigenicity assay in immunosuppressed mice

Ten 6-week old BALB/C nu/nu female nude mice were randomly divided into two groups (n=5 in each group): GL261 cells stably transfected with pDsRed2-C1 vector or pDsRed2-Trim11. Aliquots (100 μl) of 5×10^5 cells of each cell group in 25% Matrigel (BD Biosciences) were subcutaneously injected into nude mice anterior to their right and left thighs on both sides. After injection, the growth of tumor nodules was estimated with caliper at a 3-day interval. On Day 15 after injection, all mice were sacrificed. Tumors were removed and tumor weight was evaluated. The tumor volume was calculated using the formula $V = (L*W^2*\pi)/6$ (L, length; W, width).

Statistical analysis

Statistical analyses were prepared using GraphPad Prism version 5.04 (GraphPad Software). All values were presented as mean ± standard error of the mean (S.E.M.). Statistical significance was determined with simple paired t-tests of one-way ANOVA.

Supplementary Material

Refer to Web version on PubMed Central for supplementary material.

Acknowledgments

Financial support: This work was supported by research funds donated by Ralph and Suzanne Stern and the Community Foundation of Jewish Federation. This study was also supported in part by start-up funds to Dr. Bota from the University of California, Irvine and the UCI Cancer Center Award Number P30CA062203 from the National Cancer Institute.

We thank Xing Gong for the preparation of glioma primary cultures, Dr. Ronald C. Kim for the neuropathologic diagnosis of tumor samples, and Dr. Abhishek Chaturbedi for the organization of the tumor list used in the study.

References

1. Gladson CL, Prayson RA, Liu WM. The pathobiology of glioma tumors. Annu Rev Pathol. 2010; 5:33–50. [PubMed: 19737106]
2. Wen PY, Kesari S. Malignant gliomas in adults. N Engl J Med. 2008; 359:492–507. [PubMed: 18669428]
3. von Deimling A, Korshunov A, Hartmann C. The next generation of glioma biomarkers: MGMT methylation, BRAF fusions and IDH1 mutations. Brain Pathol. 2011; 21:74–87. [PubMed: 21129061]
4. Ma YH, Mentlein R, Knerlich F, Kruse ML, Mehdorn HM, Held-Feindt J. Expression of stem cell markers in human astrocytomas of different WHO grades. J Neurooncol. 2008; 86:31–45. [PubMed: 17611714]
5. Zhang M, Song T, Yang L, Chen R, Wu L, Yang Z, et al. Nestin and CD133: valuable stem cell-specific markers for determining clinical outcome of glioma patients. J Exp Clin Cancer Res. 2008; 27:85. [PubMed: 19108713]
6. Singh S, Clarke I, Terasaki M, Bonn V, Hawkins C, Squire J, et al. Identification of a cancer stem cell in human brain tumors. Cancer Res. 2003; 63:5821– 5828. [PubMed: 14522905]
7. Singh S, Hawkins C, Clarke I, Squire J, Bayani J, Hide T, et al. Identification of human brain tumour initiating cells. Nature. 2004; 432:396– 401. [PubMed: 15549107]
8. Chen J, Li Y, Yu TS, McKay RM, Burns DK, Kernie SG, et al. A restricted cell population propagates glioblastoma growth after chemotherapy. Nature. 2012
9. Bao S, Wu Q, McLendon RE, Hao Y, Shi Q, Hjelmeland AB, et al. Glioma stem cells promote radioresistance by preferential activation of the DNA damage response. Nature. 2006; 444:756–760. [PubMed: 17051156]
10. Li Z, Wang H, Eyler CE, Hjelmeland AB, Rich JN. Turning cancer stem cells inside out: an exploration of glioma stem cell signaling pathways. J Biol Chem. 2009; 284:16705–16709. [PubMed: 19286664]
11. Dey M, Ulasov IV, Tyler MA, Sonabend AM, Lesniak MS. Cancer stem cells: the final frontier for glioma virotherapy. Stem Cell Rev. 2011; 7:119–129. [PubMed: 20237963]
12. Uchida N, Buck DW, He D, Reitsma MJ, Masek M, Phan TV, et al. Direct isolation of human central nervous system stem cells. Proc Natl Acad Sci U S A. 2000; 97:14720–14725. [PubMed: 11121071]
13. Zimmerman L, Parr B, Lendahl U, Cunningham M, McKay R, Gavin B, et al. Independent regulatory elements in the nestin gene direct transgene expression to neural stem cells or muscle precursors. Neuron. 1994; 12:11–24. [PubMed: 8292356]
14. Gong X, Schwartz PH, Linskey ME, Bota DA. Neural stem/progenitors and glioma stem-like cells have differential sensitivity to chemotherapy. Neurology. 2011; 76:1126–1134. [PubMed: 21346220]
15. Schmidinger M, Linzmayer L, Becherer A, Fazeny-Doemer B, Fakhrai N, Prayer D, et al. Psychometric-and quality-of-life assessment in long-term glioblastoma survivors. J Neurooncol. 2003; 63:55–61. [PubMed: 12814255]
16. Corn BW, Wang M, Fox S, Michalski J, Purdy J, Simpson J, et al. Health related quality of life and cognitive status in patients with glioblastoma multiforme receiving escalating doses of conformal three dimensional radiation on RTOG 98-03. J Neurooncol. 2009; 95:247–257. [PubMed: 19533025]
17. Reymond A, Meroni G, Fantozzi A, Merla G, Cairo S, Luzi L, et al. The tripartite motif family identifies cell compartments. EMBO J. 2001; 20:2140–2151. [PubMed: 11331580]
18. Saurin AJ, Borden KL, Boddy MN, Freemont PS. Does this have a familiar RING? Trends Biochem Sci. 1996; 21:208–214. [PubMed: 8744354]
19. Borden KL. RING fingers and B-boxes: zinc-binding protein-protein interaction domains. Biochem Cell Biol. 1998; 76:351–358. [PubMed: 9923704]

20. Hatakeyama S. TRIM proteins and cancer. Nat Rev Cancer. 2011; 11:792–804. [PubMed: 21979307]
21. Niikura T, Hashimoto Y, Tajima H, Ishizaka M, Yamagishi Y, Kawasumi M, et al. A tripartite motif protein TRIM11 binds and destabilizes Humanin, a neuroprotective peptide against Alzheimer's disease-relevant insults. Eur J Neurosci. 2003; 17:1150–1158. [PubMed: 12670303]
22. Ishikawa H, Tachikawa H, Miura Y, Takahashi N. TRIM11 binds to and destabilizes a key component of the activator-mediated cofactor complex (ARC105) through the ubiquitin-proteasome system. FEBS Lett. 2006; 580:4784–4792. [PubMed: 16904669]
23. Tuoc TC, Stoykova A. Trim11 modulates the function of neurogenic transcription factor Pax6 through ubiquitin-proteosome system. Genes Dev. 2008; 22:1972–1986. [PubMed: 18628401]
24. Hong SJ, Chae H, Lardaro T, Hong S, Kim KS. Trim11 increases expression of dopamine beta-hydroxylase gene by interacting with Phox2b. Biochem Biophys Res Commun. 2008; 368:650–655. [PubMed: 18275850]
25. Sanai N, Alvarez-Buylla A, Berger MS. Neural stem cells and the origin of gliomas. N Engl J Med. 2005; 353:811–822. [PubMed: 16120861]
26. Schwartz PH, Bryant PJ, Fuja TJ, Su H, O'Dowd DK, Klassen H. Isolation and characterization of neural progenitor cells from post-mortem human cortex. J Neurosci Res. 2003; 74:838–851. [PubMed: 14648588]
27. Kurihara H, Zama A, Tamura M, Takeda J, Sasaki T, Takeuchi T. Glioma/glioblastoma-specific adenoviral gene expression using the nestin gene regulator. Gene Ther. 2000; 7:686–693. [PubMed: 10800092]
28. Griguer CE, Oliva CR, Gobin E, Marcorelles P, Benos DJ, Lancaster JR Jr, et al. CD133 is a marker of bioenergetic stress in human glioma. PLoS One. 2008; 3:e3655. [PubMed: 18985161]
29. Zhou XD, Wang XY, Qu FJ, Zhong YH, Lu XD, Zhao P, et al. Detection of cancer stem cells from the C6 glioma cell line. J Int Med Res. 2009; 37:503–510. [PubMed: 19383245]
30. Lim DA, Cha S, Mayo MC, Chen MH, Keles E, VandenBerg S, et al. Relationship of glioblastoma multiforme to neural stem cell regions predicts invasive and multifocal tumor phenotype. Neuro Oncol. 2007; 9:424–429. [PubMed: 17622647]
31. Rao RD, Uhm JH, Krishnan S, James CD. Genetic and signaling pathway alterations in glioblastoma: relevance to novel targeted therapies. Front Biosci. 2003; 8:e270–280. [PubMed: 12700121]
32. Roberts PJ, Der CJ. Targeting the Raf-MEK-ERK mitogen-activated protein kinase cascade for the treatment of cancer. Oncogene. 2007; 26:3291–3310. [PubMed: 17496923]
33. Schlessinger J. Cell signaling by receptor tyrosine kinases. Cell. 2000; 103:211–225. [PubMed: 11057895]
34. Eramo A, Ricci-Vitiani L, Zeuner A, Pallini R, Lotti F, Sette G, et al. Chemotherapy resistance of glioblastoma stem cells. Cell Death Differ. 2006; 13:1238–1241. [PubMed: 16456578]
35. Zhao C, Deng W, Gage FH. Mechanisms and functional implications of adult neurogenesis. Cell. 2008; 132:645–660. [PubMed: 18295581]
36. Kordes C, Sawitza I, Muller-Marbach A, Ale-Agha N, Keitel V, Klonowski-Stumpe H, et al. CD133+ hepatic stellate cells are progenitor cells. Biochem Biophys Res Commun. 2007; 352:410–417. [PubMed: 17118341]
37. Sherman JH, Redpath GT, Redick JA, Purow BW, Laws ER, Jane JA Jr, et al. A novel fixative for immunofluorescence staining of CD133-positive glioblastoma stem cells. J Neurosci Methods. 2011; 198:99–102. [PubMed: 21402102]
38. Fredens K, Dahl R, Venge P. An immunofluorescent method for a specific demonstration of granulocytes and some of their proteins (ECP and CCP). Histochemistry. 1986; 84:247–250. [PubMed: 3519546]
39. Bigner SH, Humphrey PA, Wong AJ, Vogelstein B, Mark J, Friedman HS, et al. Characterization of the epidermal growth factor receptor in human glioma cell lines and xenografts. Cancer Res. 1990; 50:8017–8022. [PubMed: 2253244]
40. Raab G, Klagsbrun M. Heparin-binding EGF-like growth factor. Biochim Biophys Acta. 1997; 1333:F179–199. [PubMed: 9426203]

41. Suo Z, Risberg B, Karlsson MG, Villman K, Skovlund E, Nesland JM. The expression of EGFR family ligands in breast carcinomas. Int J Surg Pathol. 2002; 10:91–99. [PubMed: 12075402]

42. Tarbe N, Losch S, Burtscher H, Jarsch M, Weidle UH. Identification of rat pancreatic carcinoma genes associated with lymphogenous metastasis. Anticancer Res. 2002; 22:2015–2027. [PubMed: 12174879]

43. Mishima K, Higashiyama S, Asai A, Yamaoka K, Nagashima Y, Taniguchi N, et al. Heparin-binding epidermal growth factor-like growth factor stimulates mitogenic signaling and is highly expressed in human malignant gliomas. Acta Neuropathol. 1998; 96:322–328. [PubMed: 9796995]

44. McCarthy SA, Samuels ML, Pritchard CA, Abraham JA, McMahon M. Rapid induction of heparin-binding epidermal growth factor/diphtheria toxin receptor expression by Raf and Ras oncogenes. Genes Dev. 1995; 9:1953–1964. [PubMed: 7649477]

45. Ongusaha PP, Kwak JC, Zwible AJ, Macip S, Higashiyama S, Taniguchi N, et al. HB-EGF is a potent inducer of tumor growth and angiogenesis. Cancer Res. 2004; 64:5283–5290. [PubMed: 15289334]

46. Pistollato F, Chen H-L, Rood BR, Zhang H-Z, D'Avella D, Denaro L, et al. Hypoxia and HIF1alpha Repress the Differentiative Effects of BMPs in High-Grade Glioma. Stem Cells. 2009; 27:7–17. [PubMed: 18832593]

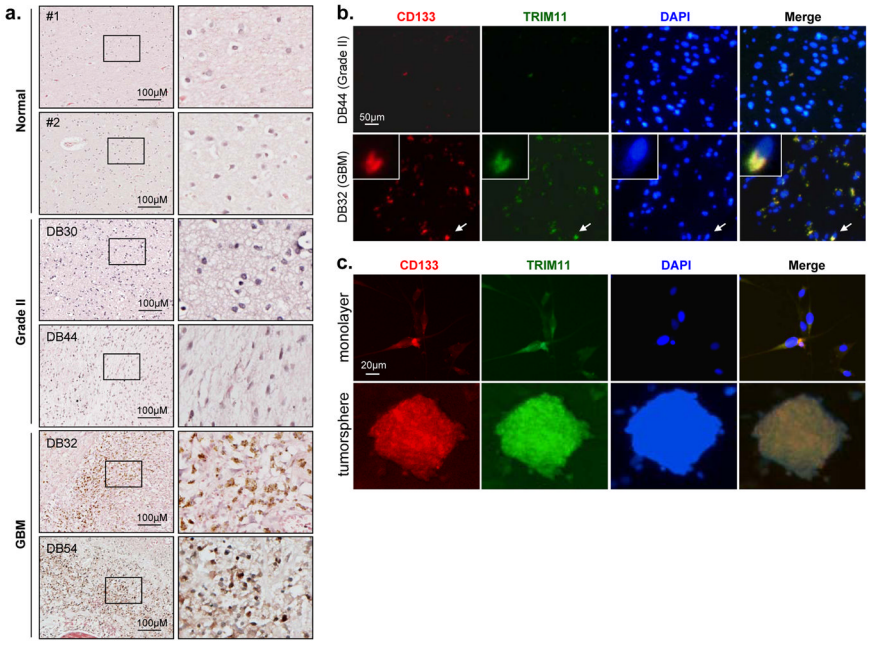

Figure 1.

TRIM11 is enriched in GBM tissues as well as high-grade glioma-derived GSCs. (**a**) Immunohistochemical staining for TRIM11 in human normal brains, Grade II (DB30 and DB44) and GBM (DB32 and DB54) surgical biopsies. (**b**) Immunofluorescent staining for CD133 (red) and TRIM11 (green) in DB44 and DB32 surgical biopsies. (**c**) Immunofluorescent staining of endogenously expressed CD133 and TRIM11 on monolayer (top) and budding tumorsphere (bottom) of HuTuP01-GSC. Nuclei were counterstained with DAPI (blue).

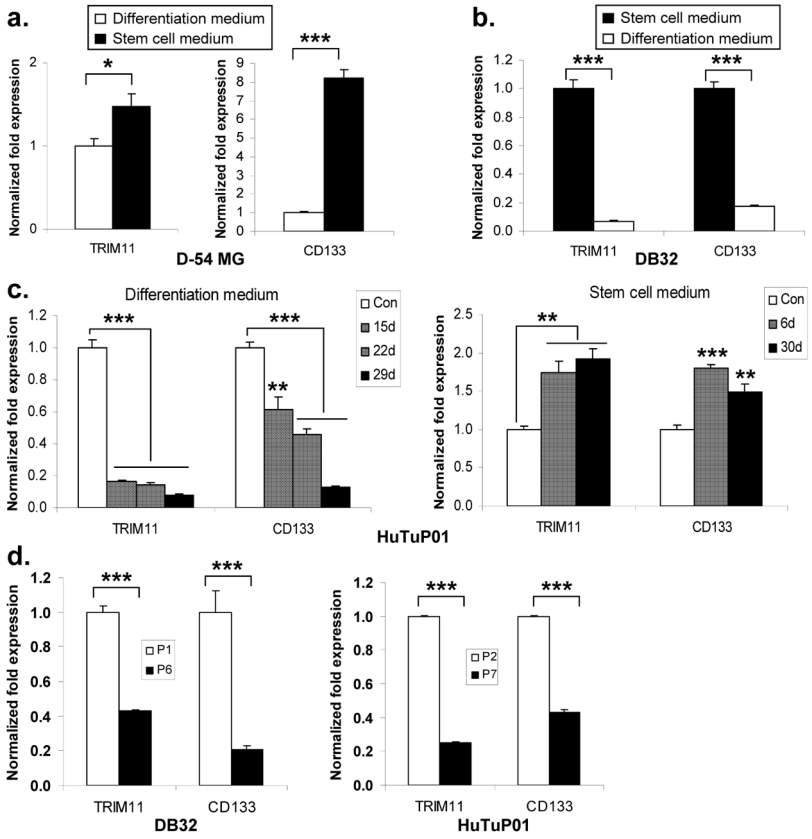

Figure 2.

TRIM11 mRNA levels correlate with differentiation status and *CD133* mRNA levels in malignant glioma cells. (**a**) D-45 MG cells were cultured in stem cell medium for 1 month and RNA was isolated. (**b**) DB32-GSC was cultured with differentiation medium for 1 month and RNA was isolated. (**c**) HuTuP01-GSC was cultured with differentiation medium for different time points and switched back to stem cell medium followed by RNA isolation at the indicated time points. (**d**) Early and late passages of DB32-GSC and HuTuP01-GSC were collected and RNA was isolated. qRT-PCR was then performed to measure the mRNA levels of *TRIM11* and *CD133*, and *ACTB* was an internal control. $*p < 0.05$, $**p < 0.01$, $***p < 0.001$.

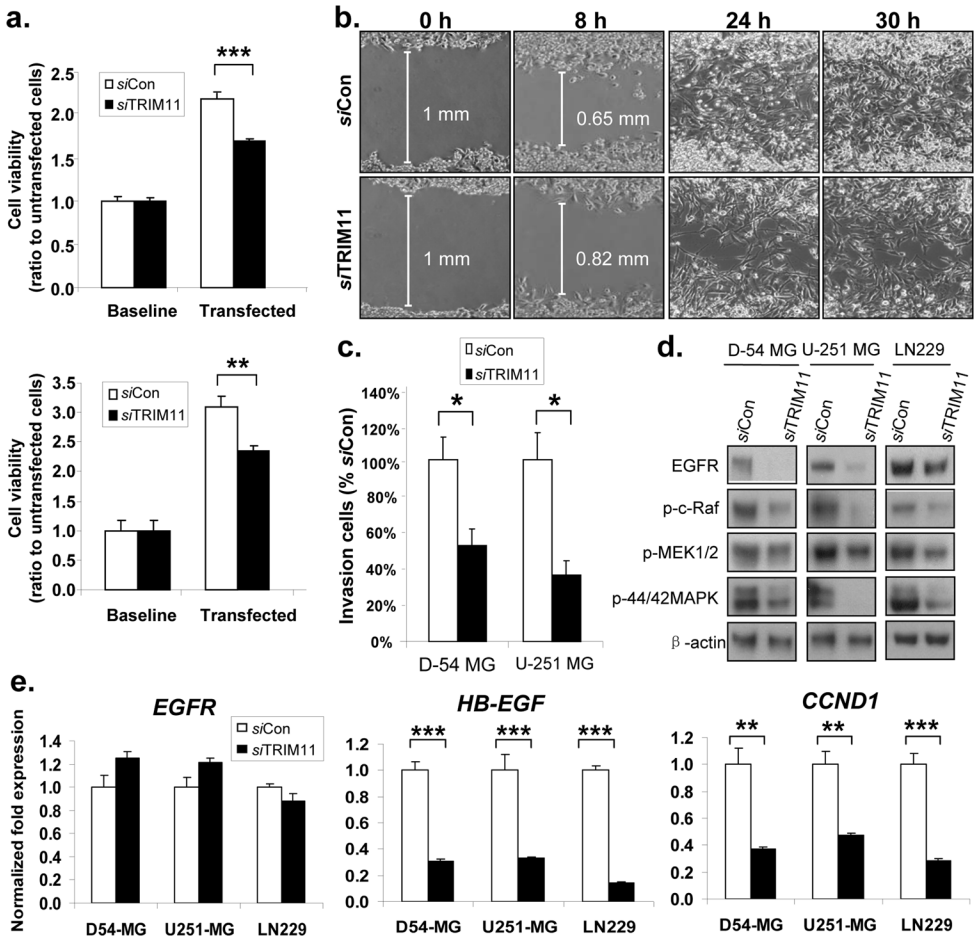

Figure 3.

TRIM11 down-regulation inhibits cell proliferation, migration, invasion, EGFR/MAPKs signaling pathway as well as transcription of *HB-EGF* and *CCND1*. (**a**) The effect of TRIM11 knockdown on D-54 cell growth rate was measured by MTT assay (upper panel) and BrdU incorporation analysis (lower panel) in *si*Con and *si*TRIM11 (*si*-4) transfectants. Data were the ratio of the absorbance of transfected cells to that of untransfected (baseline) cells. (**b**) Wound closure assay was performed using *si*TRIM11 (*si*-4) or *si*Con transfectants of U-251. The time required for 'wound closure' was monitored and photographed at indicated time points. (**c**) Invasion activity of the transfectants was analyzed by using Matrigel Invasion chambers. The summary of the invasion assay was showed in percent. (**d**) The effect of TRIM11 suppression by *si*TRIM11 (*si*-4) on the expression of EGFR, phospho-c-Raf, phospho-MEK1/2 and phospho-44/42MAPK were analyzed by Western blotting. (**e**) qRT-PCR was performed to compare the mRNA levels of *EGFR* (left), *HB-EGF* (middle) and *CCND1* (right) between *si*TRIM11 (*si*-4) or *si*Con transfectants, and *ACTB* was an internal control. *$p < 0.05$, **$p < 0.01$, ***$p < 0.001$.

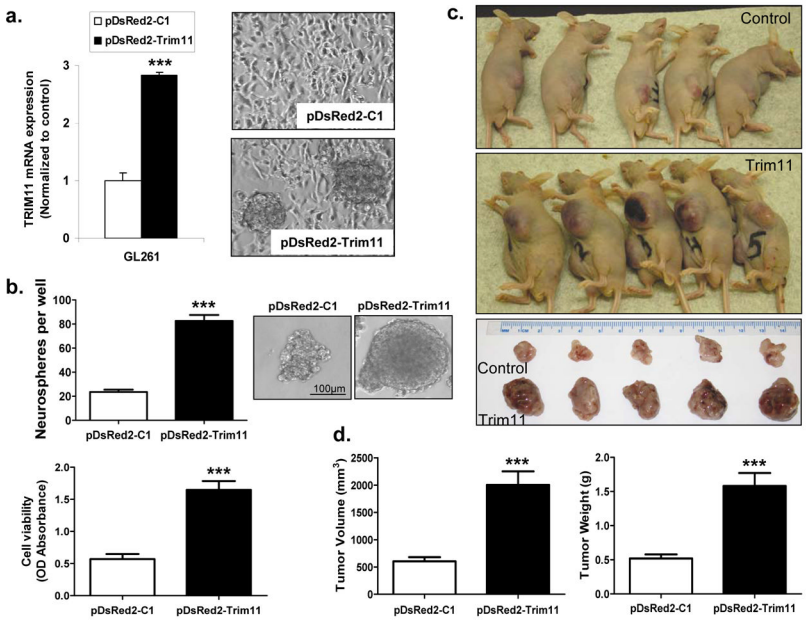

Figure 4.

Over-expression of TRIM11 promotes tumorsphere formation and proliferation *in vitro* and tumor growth *in vivo*. (**a**) Stable over-expression of TRIM11 in mouse GL261 cells was achieved by transfection of pDsRed2-Trim11 vector, and followed by G418 selection. Expression of *TRIM11* mRNA was analyzed by qRT-PCR and normalized to expression of *ACTB*. The morphology of stable transfectants was shown on right. Tumorspheres can be detected in pDsRed2-Trim11 cells. (**b**) Overexpression of TRIM11 promoted tumorsphere formation (upper panel), and representative images of tumorspheres derived from GL261 stable transfectants were shown on right. Increased proliferation was found in pDsRed2-Trim11 cells when cultured on Matrigel-coated surface (lower panel). (**c**) GL261 cells stably transfected with pDsRed2-Trim11 or a control vector were injected s.c. into nude mice. Fifteen days after the injection, mice were sacrificed and photographed. (**d**) Tumor volume (left) and weight (right) were measured. ***$p < 0.001$.

Table 1

Brain tumors used in study and the expression fold change of *TRIM11*, *CD133* and *Nestin* (related to Supplementary Figure 1a).

Category	Grade	Code	Tumor type	Sex	Age	Survival* (months)	*TRIM11* (± SEM)	*CD133* (± SEM)	*Nestin* (± SEM)
Malignant glioma stable cell lines		U-251 MG					1.00 ± 0.03	1.00 ± 0.11	32.81 ± 3.77
		D-54 MG					1.74 ± 0.09	0.37 ± 0.03	1.00 ± 0.16
		LN229					1.78 ± 0.29	0.22 ± 0.04	0.10 ± 0.02
		U-87 MG					0.83 ± 0.07	0.43 ± 0.04	1.15± 0.13
Glioma stem-like cells	**II**	DB29	Oligodendroglioma	male	73	Alive (>27)	0.71 ± 0.02	0.02 ± 0.01	11.28 ± 0.55
		DB30	Oligodendroglioma	female	52	Alive (>26)	1.45 ± 0.13	0.10 ± 0.01	2.93 ± 0.26
		DB39	Oligodendroglioma	male	44	Alive (>21)	1.01 ± 0.09	1.07 ± 0.14	3.88 ± 0.18
		DB43	Oligodendroglioma	male	49	#	1.35 ± 0.09	0.36 ± 0.05	2.97 ± 0.18
		DB44	Oligodendroglioma	male	32	Alive (>19)	0.75 ± 0.07	0.64 ± 0.05	3.42 ± 0.03
		DB51	Oligodendroglioma	male	75	Alive (>15)	7.29 ± 0.23	17.75 ± 2.52	8.85 ± 0.16
		DB55	Oligodendroglioma	male	23	Alive (>13)	1.53 ± 0.09	1.39 ±.60	35.40 ± 2.79
	III	DB26	Oligodendroglioma	male	71	14	1.48 ± 0.04	0.23 ± 0.13	5.03 ± 0.59
		DB33	Oligodendroglioma	male	24	10	3.59 ± 0.31	6.65 ± 1.43	2.30 ± 0.37
		DB47	Oligoastrocytoma	male	30	11	2.20 ± 0.08	0.58 ± 0.03	24.18 ± 1.42
	GBM	DB17	Glioblastoma	female	32	8	3.26 ± 0.17	11.22 ± 0.89	10.29 ± 0.89
		DB32	Glioblastoma	female	53	9	29.25 ± 3.38	67.07 ± 4.61	22.60 ± 4.63
		DB34	Glioblastoma	female	61	9	4.08 ± 0.90	3.77 ± 1.11	16.95 ± 4.08
		DB37	Glioblastoma	female	73	13	0.89 ± 0.03	3.83 ± 0.26	37.02 ± 2.23
		DB49	Glioblastoma	male	18	4	2.68 ± 0.09	6.65 ± 0.66	30.26 ± 1.54
		DB50	Glioblastoma	male	61	14	1.67 ± 0.07	4.54 ± 0.52	24.29 ± 0.78
		DB53	Glioblastoma	male	61	7	2.81 ± 0.05	3.48 ± 0.67	8.80 ± 0.56
		DB54	Glioblastoma	male	26	7	3.64 ± 0.08	13.15 ± 1.75	58.44 ± 1.38
		HuTuP01	Glioblastoma	male	64	N/A	13.78 ± 0.49	27.34 ± 3.09	19.87 ± 2.22
Neural stem/progenitor cells		SC23					1.10 ± 0.05	1480.05 ± 15.98	79.72 ± 5.41
		SC27					2.04 ± 0.06	2942.04 ± 0.06	99.65 ± 10.22
		SC30					0.35 ± 0.02	787.16 ± 51.34	55.64 ± 1.86

* Survival from surgery to death

Dead unrelated to tumor progression

Table 2

Human EGF/PDGF Signaling PCR Array analysis in control and TRIM11 knockdown cells (fold change ≥ 2).

			D-54 MG	U-251 MG
Gene name	**Gene symbol**	**Accession no.**	**Fold change (≥ 2) (siCon *vs.* siTRIM11)**	**Fold change (≥ 2) (siCon *vs.* siTRIM11)**
Collagen, type I, alpha 1	COL1A1	NM_000088	2.2665	
Fibronectin 1	FN1	NM_002026	3.5469	
Matrix metallopeptidase 7 (matrilysin, uterine)	MMP7	NM_002423	2.1534	
Protein kinase C, alpha	PRKCA	NM_002737	2.2441	
Signal transducer and activator of transcription 1	STAT1	NM_007315	2.4457	
Tumor protein p53	TP53	NM_000546	2.288	
Cyclin D1	CCND1	NM_053056	−2.6441	−2.8061
Dual specificity phosphatase 6	DUSP6	NM_001946	−2.2812	
Early growth response 1	EGR1	NM_001964	−2.3354	
Heparin-binding EGF-like growth factor	HBEGF	NM_001945	−2.1453	−2.6983
Lymphotoxin alpha (TNF superfamily, member 1)	LTA	NM_000595	−2.8202	
V-fos FBJ murine osteosarcoma viral oncogene homolog	FOS	NM_005252		2.0096
B-cell CLL/lymphoma 2	BCL2	NM_000633		−2.0404
Fas ligand (TNF superfamily, member 6)	FASLG	NM_000639		−5.666

Note: Human EGF/PDGF Signaling PCR Array was performed to compare gene expression changes by TRIM11 downregulation.

Genes with greater than 2 fold regulation were considered as significant difference.